Pore Structure and Swelling Behavior of Porous Hydrogels Prepared via a Thermal Reverse-Casting Technique

Aurelio Salerno, Rossella Borzacchiello, Paolo A. Netti

Interdisciplinary Research Centre on Biomaterials (CRIB), University of Naples Federico II and Centre for Advanced Biomaterials for Health Cared (IIT@CRIB), Istituto Italiano di tecnologia, Piazzale Tecchio 80, 80125 Naples, Italy

Received 28 April 2011; accepted 28 April 2011
DOI 10.1002/app.34778
Published online 11 August 2011 in Wiley Online Library (wileyonlinelibrary.com).

ABSTRACT: In this work, we investigated the design and fabrication of porous polyacrylamide hydrogels via a thermal reverse-casting technique. The porous hydrogels were prepared by the free-radical crosslinking polymerization of the monomer solution within the space of an agarose gel, which after the setting of the chemical gel, was removed to allow for the formation of an interconnected porosity pathway. Two different agarose/monomer solution ratios were selected to modulate the porosity of the hydrogels, and the as-obtained samples were characterized in terms of their chemical structure, morphology, thermal properties, and swelling behavior in different ionic strength solutions. The results of this study demonstrate that the reverse-casting process enhanced the solvent-retaining capability of the hydrogels and that their swelling ratio increased with increasing concentration of the agarose solution in the initial formulation. All of these results finally demonstrate that the pore structure features played a key role in defining the swelling behavior of the hydrogels. © 2011 Wiley Periodicals, Inc. J Appl Polym Sci 122: 3651–3660, 2011

Key words: hydrogels; macroporous polymers; microstructure; swelling

INTRODUCTION

Polymeric hydrogels are materials composed of hydrophilic crosslinked polymer chains, which are either of synthetic or natural origin, able to absorb and retain large amounts of water. Hydrogels have the peculiarity of undergoing reversible and discontinuous volume changes in response to variations in the external conditions, such as the solvent composition, temperature, salt concentration, and pH.[1–4] The possibility of fine-tuning the swelling properties of polymeric hydrogels in response to a specific external environment is a great advantage for several applications, such as for the design of smart materials, separation membranes, and biocompatible and biodegradable scaffolds for tissue engineering.[3,4–6]

Polyelectrolyte hydrogels are a class of materials in which the polymer chains provide acid and basic bound groups that interact electrostatically with each other or with the mobile charges eventually present in the external solution.[7–9] This feature may significantly improve the swelling properties of the hydrogel and may promote and guide specific interactions with polarized biological molecules, such as collagen, biotin, and insulin, when they are used for biomedical application purposes.[8,9]

Recently, it has been reported that the creation of interconnected porosity networks within polymeric hydrogels may improve their performance.[10,11] Indeed, the presence of a three-dimensional porous pathway within a hydrogel material may reduce the solvent-transport resistance, as a consequence of solvent flow by convection, a faster process when compared to simple diffusion.[10] Furthermore, the possibility of accurately designing the pore structure features of the hydrogels, especially in terms of the porosity and pore size distribution, is strongly needed for tissue engineering applications, to allow for the three-dimensional cell and tissue infiltration.[5,12]

A large number of strategies have been proposed to produce porous polymeric hydrogels.[6,12–15] These include foaming techniques,[12] phase separation,[13] *in situ* crosslinking polymerization,[6] particulate leaching,[13] freeze drying,[14] and reverse casting.[15] Porous hydrogels starting from different polymeric materials and with well-controlled porosities and pore size distributions have been obtained with these approaches. Furthermore, the results reported in these studies indicate that the swelling capability of porous hydrogels is significantly affected by the topological features of the porous network, mainly the void fraction and the pore size and interconnectivity. For instance, Sannino et al.[12] reported that the swelling properties

Correspondence to: P. A. Netti (nettipa@unina.it).

of poly(ethylene glycol) hydrogels prepared by CO_2 as a foaming agent increased with increasing interconnectivity of the pore structure because of the enhanced capillary diffusion of the solvent. Furthermore, Přádný et al.[13] showed that the degradation rate of porous polyhudroxyethyl methacrylate (PHEMA) hydrogels increased with the increase of the total pore surface area of the hydrogels because the hydrolytic agent had easier access to the crosslinks between macromolecules, and thus, the time required for degradation decreased.

Along these research lines, in this study, we report the fabrication of novel porous polyacrylamide hydrogels by a reverse-casting technique; we critically investigated the effects of the pore structure features of the hydrogels, mainly the morphology and pore size distribution, on their swelling behavior in different ionic strength (IS) solutions. The polyacrylamide hydrogels were synthesized by a free-radical crosslinking polymerization. Furthermore, to allow for the formation of the porous network within the hydrogels, the polymerization process was performed within the space of a thermoreversible agarose gel. which, after the setting of the chemical gel, was selectively removed, which left an interconnected porosity pathway.

The chemical composition, thermal properties, and morphology of the obtained hydrogels were assessed by attenuated total reflection (ATR) spectroscopy, thermogravimetric analysis (TGA), derivative TGA, differential scanning calorimetry (DSC), and scanning electron microscopy (SEM). Furthermore, we carried out swelling tests by soaking the hydrogels in water solutions at different ISs, and the results were correlated to the microstructural properties of the hydrogels at equilibrium swelling.

EXPERIMENTAL

Materials

Sodium methacrylate and *N,N*-methylene bisacrylamide were used for the free-radical crosslinking polymerization. Methacrylamidopropyltrimethyl ammonium chloride and ammonium persulfate were selected as the cationic comonomer and initiator, respectively. Agarose powder (type III-A) was used for the preparation of the templating hydrogel. All of the chemicals were purchased from Sigma-Aldrich (Milan, Italy) and were used as received.

Preparation of the hydrogels

The nonporous sodium methacrylate (SM) hydrogel was synthesized by the mixture 17 mL of a water solution containing 0.4% w/v sodium methacrylate, 8×10^{-4}% w/v *N,N*-methylene bisacrylamide, and 0.3% v/v methacrylamidopropyltrimethyl ammonium chloride with 5 mL of a water solution containing 9.7×10^{-4}% w/v ammonium persulfate. The mixing process was performed for 5 min at room temperature (RT) with a magnetic stirrer. The as-obtained solution was finally stored at 70°C for 3 h to allow for the free-radical crosslinking polymerization.

As shown in Figure 1, the preparation of porous agarose-sodium methacrylate (SMA) hydrogels was performed by a three-step process: (1) a water solution containing 2×10^{-2} w/v of agarose at 90°C was mixed with the monomer solution for 1 min at RT, after which the agarose gelification was induced by a decrease in the temperature of the system to RT; (2) the as-obtained gel was subsequently subjected to thermal treatment at 70°C for 3 h to allow for the free-radical crosslinking copolymerization of the reactive monomer solution; and (3) the agarose was finally removed in water at 90°C to induce the formation of porosity within the polyacrylamide hydrogel.

Two different agarose/monomer solution volume ratios were used to control the sample's pore structure: agarose-sodium methacrylate 0.5 ($SMA_{0.5}$) was obtained with an agarose/monomer solution ratio equal to 0.5, whereas agarose-sodium methacrylate 0.25 ($SMA_{0.25}$) was obtained with an agarose/monomer solutions ratio equal to 0.25.

Characterization of the hydrogels in dry conditions

ATR spectroscopic measurements were performed on SM, $SMA_{0.25}$, and $SMA_{0.5}$ hydrogels in dry conditions with a Necsus-Nicolet spectrophotometer (Milan, Italy), with the collection of 32 scans for each sample at a resolution of 1 cm^{-1}. Before the test, the samples were compression-molded at RT and 30 bar to prepare the 50 μm thick films.

TGA/derivative TGA and DSC were performed to evaluate the effect of the templating process on the thermal properties of the hydrogels. In particular, TGA experiments were carried out on a TGA 2950 (TA Instruments, Milan, Italy) over a temperature range of 30–700°C and at 10°C/min under an inert atmosphere. Samples weighing 10 mg were used for the test.

For DSC analysis, samples, 5 mg each, were first heated to 110°C at 10°C/min and maintained at this temperature for 5 min to eliminate the residual water. Then, the temperature was reduced to −60°C, and the samples were reheated up to 50°C at 2°C/min to evaluate the glass-transition temperature (T_g).

The morphology of the hydrogels was evaluated by means of SEM (S440, Leica, Wetzlar, Germany). The surface of the samples were gold-sputtered and analyzed at an accelerating voltage of 20 kV.

For swelling characterization, the samples were dried at ambient pressure and soaked in different IS

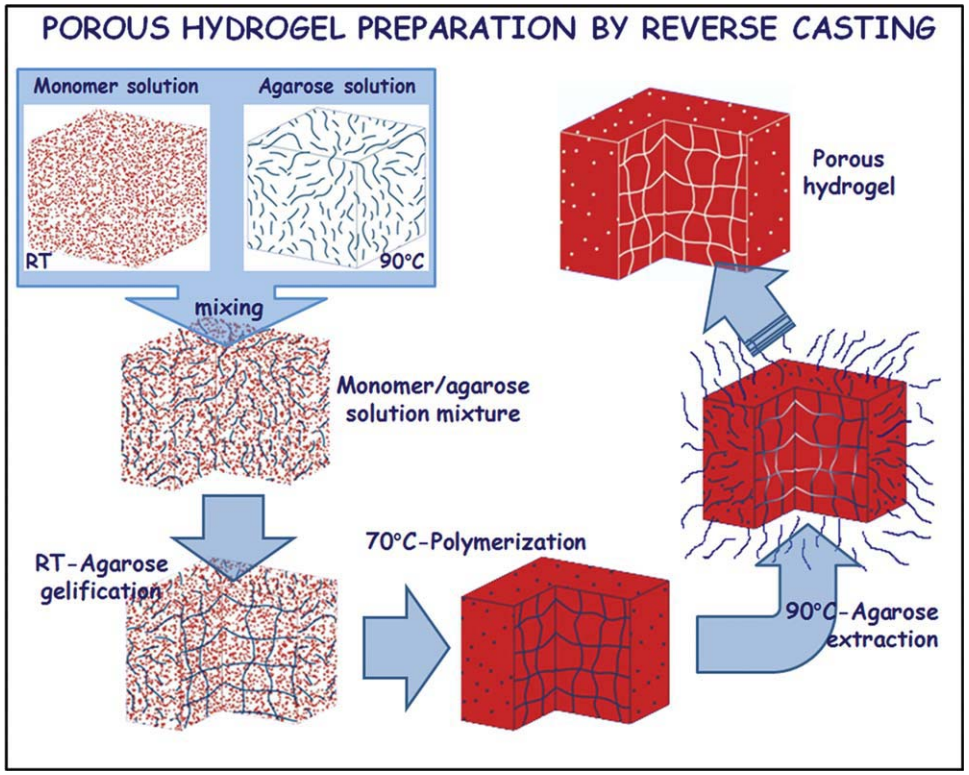

Figure 1 Scheme of the reverse-casting process used for the preparation of the porous hydrogels. [Color figure can be viewed in the online issue, which is available at wileyonlinelibrary.com.]

solutions, in the range from 10^{-7} to 10^{-1} mol/L, at RT. The solutions were prepared by the addition of different concentrations of NaCl in distilled water. At different soaking times, the hydrogels were extracted from the solution, rolled on an aluminum paper to remove the unabsorbed water, and weighed on an analytical balance (AB104-S, Mettler Toledo, Milan, Italy) to assess the weight gain. The swelling ratio was finally evaluated as the ratio between the wet weight (m_W) and dry weight (m_D) of the sample. Swelling tests were performed until the measured weight change of the samples was lower than 1% for at least 4 days. During the sorption stages, the water was continuously changed to avoid variation of the IS of the solution. Each measurement was performed in triplicate.

Characterization of the hydrogels in wet conditions

TGA and DSC analyses were performed on the wet samples to evaluate the amount of freezable and nonfreezable water within the hydrogels at equilibrium swelling. For the TGA experiments, samples weighing 10 mg were tested over a 30–300°C temperature range at 10°C/min under an inert atmosphere. DSC experiments were carried out in the −50 to 50°C temperature range, and the samples were tested at a temperature scan rate of 2°C/min under an inert atmosphere. The evaluation of the freezable and nonfreezable water was performed as described by Li et al.[16] in a previous work.

The morphology of the swollen hydrogels was evaluated by SEM analysis. The samples were freeze-dried overnight and analyzed by SEM. Image (Image J , NIH, free software; http://rsb.info.nih.gov/ij) analysis was carried out to evaluate the pore size distribution and the mean pore size of the porous hydrogels. For this test, the SEM micrographs were converted first to binary images, which indicated separately the bulk (white) and the void (black) phases. The as-obtained binary images were further analyzed by Image J software, which enabled us to measure the pore size distribution and mean size. At least 100 pores for each hydrogel were measured, and the pore size was determined according to ASTM D 3576.

RESULTS

As shown in the scheme of Figure 1, the reverse-casting technique used for the fabrication of the porous polyacrylamide hydrogels involved three main steps: (1) the creation of a physical gel by the mixture of the monomer solution with the agarose solution, (2) the polymerization of the monomer solution and the formation of an interpenetrated system, and (3) the selective dissolution of the agarose to induce the formation of an interconnected porous pathway within the settled gel.

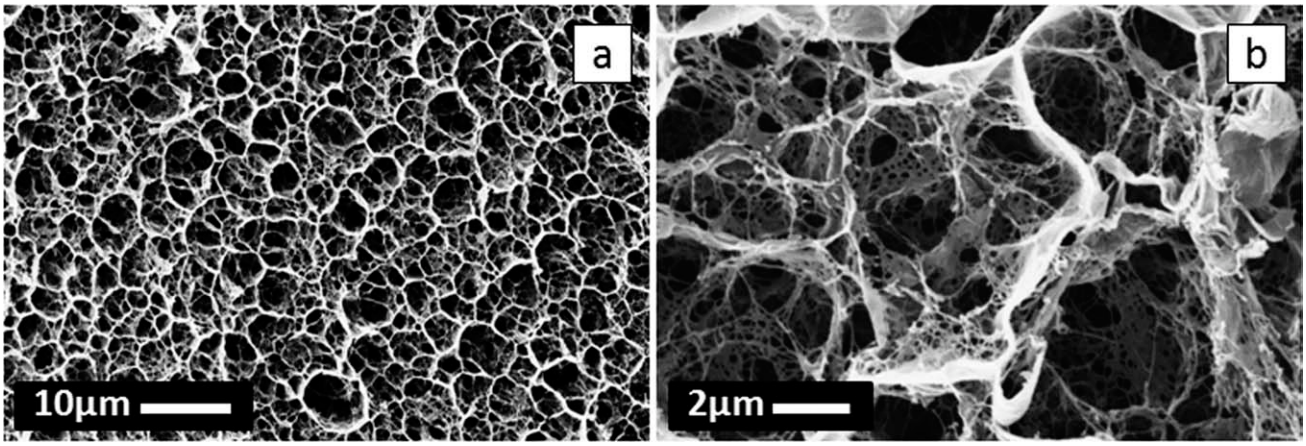

Figure 2 (a) Low- and (b) high-magnification SEM micrographs of the agarose hydrogels.

The selection of the agarose gel for the reverse-casting process mainly relied on its morphological and thermal properties. In particular, as reported in the SEM micrographs of Figure 2, the agarose gel was characterized by an interconnected pore structure, suitable to accommodate the monomer solution during the mixing and crosslinking processes. Furthermore, when mixed with the monomer solution, the agarose allowed for the creation of an interpenetrated system that was thermally stable during the polymerization process[17] and that could be selectively extracted from the settled gel to create the porous network.[15]

Physical and chemical characterization of the dry hydrogels

Figure 3 reports the ATR spectra of the SM, $SMA_{0.25}$, and $SMA_{0.5}$ samples. The spectra of SM was characterized by the typical stretching vibration of amide II groups at 1650 cm^{-1} (C=O) and at 1542 and 1478 cm^{-1} (N—H). The stretching vibration of S=O groups was observed at 1403 and 1205 cm^{-1}, whereas the peaks at 1340 and 966 cm^{-1} were ascribable to C—H and CH_2=CH stretching, respectively. Minor differences were observed by comparison of the SM spectrum with the spectra of the $SMA_{0.25}$ and $SMA_{0.5}$ hydrogels; this comparison indicated that the chemical composition of the hydrogels was not significantly affected by the reverse-casting process.

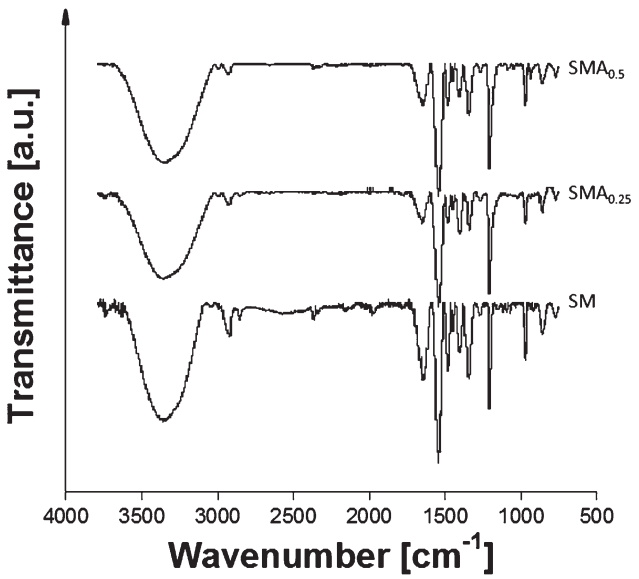

Figure 3 ATR spectra of the SM, $SMA_{0.25}$, and $SMA_{0.5}$ hydrogels.

The results of the thermal characterization of the hydrogels in the dry state are reported in Table I. As shown, all of the samples evidenced three main thermal degradation steps, which were in the temperature ranges 40–160, 180–250, and 350–460°C. The first weight loss, equal to 20%, was related to the evaporation of the residual (bound) water from the hydrogels and characterized by a peak temperature (T_{d1}) of 110°C. The degradation of the amidic groups of the gels was responsible for the second weight loss observed, which was equal to 15%, and the correspondent T_{d2} was in the range from 185 to 195°C. All of the hydrogels were completely degraded at the final temperature investigated, and this degradation process was characterized by a T_{d3} in the range from 415 to 426°C.

Differences were observed for the T_g values of the hydrogels, as evaluated by the DSC test. In particular, T_g progressively decreased from 2.1°C for neat SM to −6.8°C for $SMA_{0.5}$ (Table I).

TABLE I
Results of the TGA and DSC Characterizations Performed on the Dry Hydrogels

Sample	T_{d1} (°)	T_{d2} (°)	T_{d3} (°)	T_g (°)
SM	110.6	195.3	426.1	2.1
$SMA_{0.25}$	108.9	193.6	419.4	−3.3
$SMA_{0.5}$	108.5	186.3	415.6	−6.8

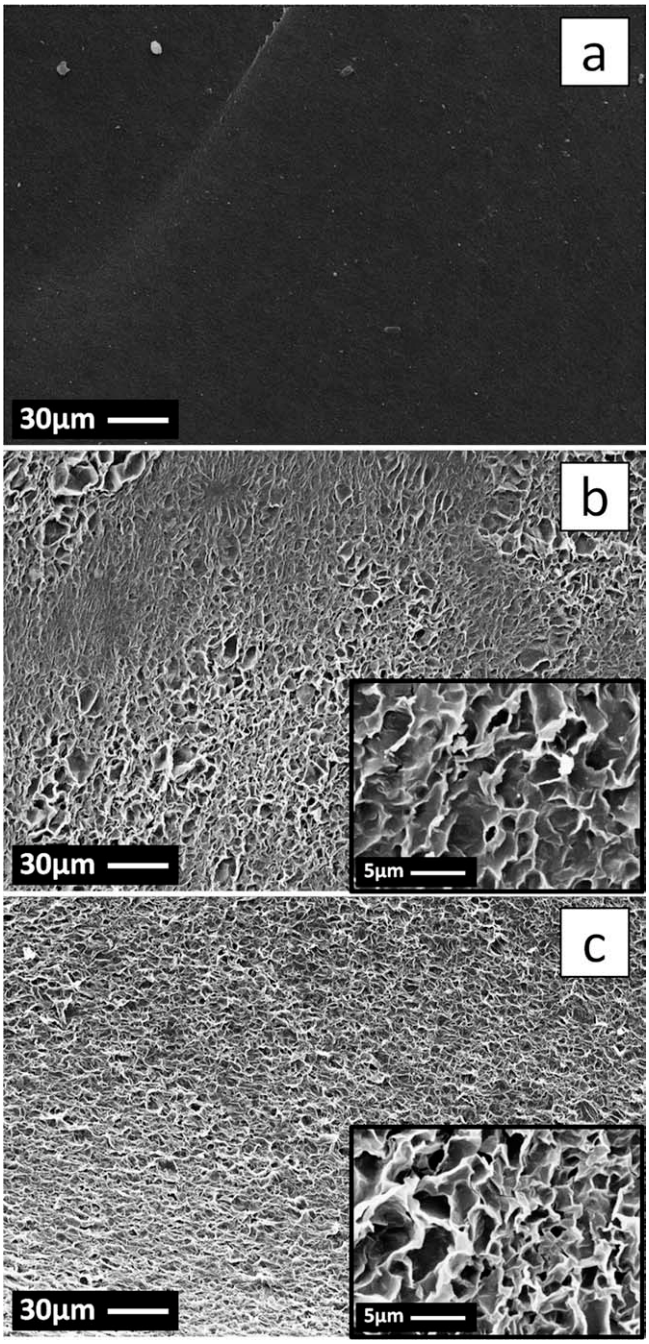

Figure 4 Morphology of the (a) SM, (b) $SMA_{0.25}$, and (c) $SMA_{0.5}$ air-dried hydrogels.

Figure 4 reports the morphology of the surface of the hydrogels. As expected, SM was characterized by a nonporous surface [Fig. 4(a)], whereas a spongelike morphology was observable for both the $SMA_{0.25}$ and $SMA_{0.5}$ hydrogels, and slight differences were observed with respect to the concentration of the agarose [Figs. 4(b,c), respectively].

Swelling tests were carried out on the SM, $SMA_{0.25}$, and $SMA_{0.5}$ hydrogels in water at RT and with different ISs. The results of these tests are reported in Figure 5 and indicate that both hydrogel formulation and IS had a great impact on the swelling of the samples. Indeed, we observed a decrease of the swelling ratio of SM, $SMA_{0.25}$, and $SMA_{0.5}$ with the increase of the IS of the soaking solution (Fig. 5) and an increase of the swelling ratio after the reverse-casting process for all of the ISs investigated. In particular, the highest swelling, equal to 270, was observed for $SMA_{0.5}$ at IS $= 10^{-7}$ mol/L, whereas a value four times lower was achieved for neat SM at the same testing conditions [Fig. 5(d)].

Thermal and microstructural characterization of swollen hydrogels

Thermal and morphological characterizations were performed on the swollen hydrogels at the equilibrium to assess the correlations between the absorption properties of the samples and their morphology and pore structure.

Table II reports the results of the TGA and DSC analyses. As shown, the weight loss in the 30–150°C temperature range increased with the increase of the agarose solution concentration, from 98.1% for neat SM to 99.6% for $SMA_{0.5}$; this clearly indicated that the reverse-casting process enhanced the water absorption capability of the hydrogels, as also observed in Figure 5. The DSC data reported in Table II also provided important information about the water absorption within the different hydrogels. In particular, the freezing temperature (T_f) increased from 2.36°C for neat SM to 0.28°C for $SMA_{0.5}$. Concomitantly, the ice-melting enthalpy (ΔH_m), obtained by integration of the DSC ice-melting peak, increased from 307.4 J/g for neat SM to 330.3 J/g for $SMA_{0.5}$. The TGA and DSC results also allowed us to quantify the weight ratios of freezable water (W^f_{H2O}) and nonfreezable water (W^b_{H2O}) with respect to the weight of the dry hydrogel (W_G).[16] In agreement with the swelling results of Figure 5, W^f_{H2O}/W_G increased with the increase of agarose solution concentration, from 61.2 for neat SM to 264.1 for $SMA_{0.5}$, as evaluated by the DSC data. The concomitant W^b_{H2O}/W_G decreased 2–3 times after the reverse-casting process.

Figure 6 reports the morphology of the swollen hydrogels at IS $= 10^{-7}$ mol/L and at equilibrium. The SM showed a nonporous surface [Fig. 6(a)], whereas a uniform porosity pattern was observable for both $SMA_{0.25}$ and $SMA_{0.5}$ [Figs. 6(b,c), respectively]. The SEM analysis also showed that the extent and size of the pores of the hydrogels increased from $SMA_{0.25}$ to $SMA_{0.5}$. This consideration was supported by the results of the morphology, pore size distribution, and mean pore size of the $SMA_{0.25}$ and $SMA_{0.5}$ swollen hydrogels in different IS solutions, reported in Figures 7 and 8. Indeed, both hydrogels showed uniform morphologies

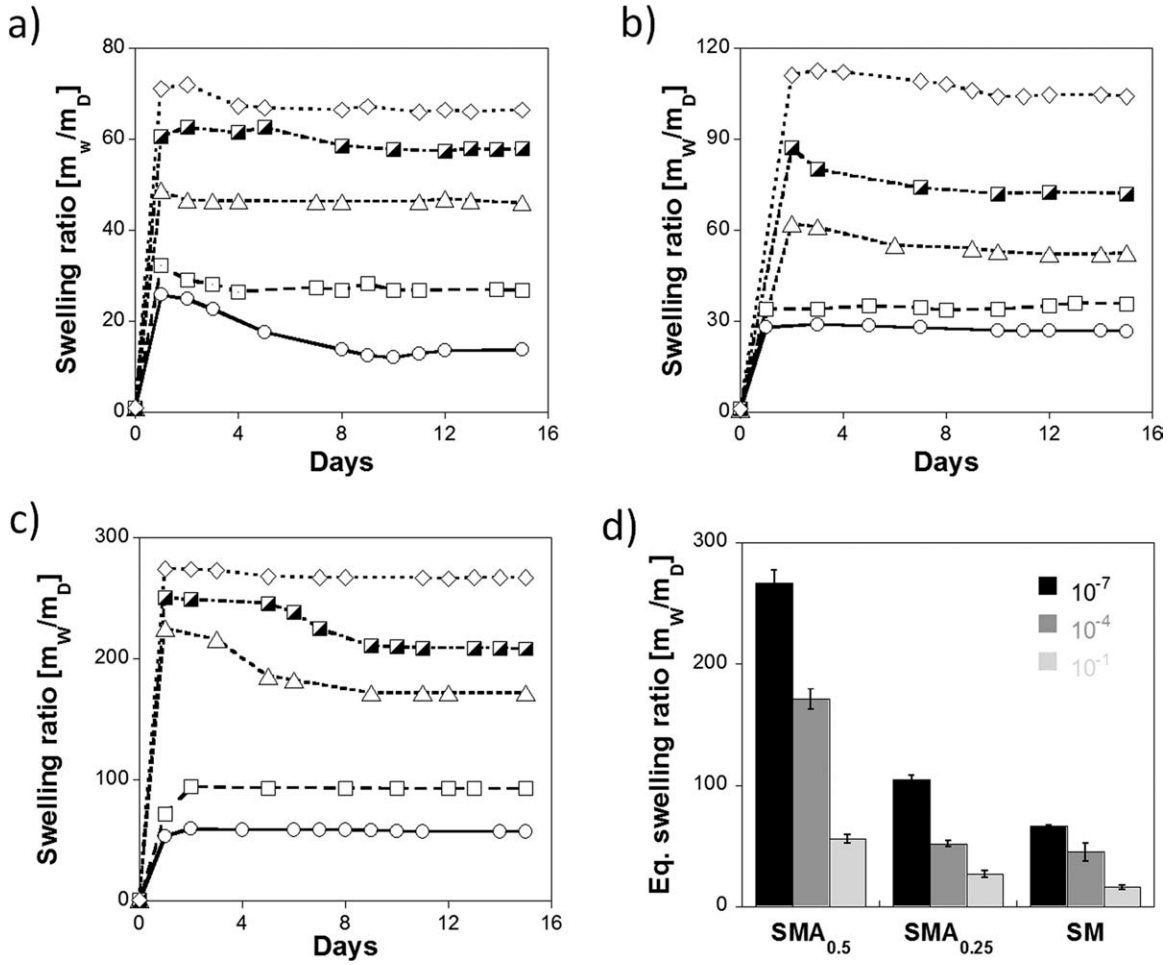

Figure 5 Effect of the IS of the solution on the swelling of the (a) SM, (b) $SMA_{0.25}$, and (c) $SMA_{0.5}$ hydrogels over time and (d) comparison between the equilibrium swelling of the hydrogels under different IS solutions.

(Fig. 7), with $SMA_{0.5}$ characterized by larger pores compared to $SMA_{0.25}$. This effect was observed for all of the ISs investigated during the swelling tests.

In agreement with the swelling results of Figures 5 and 7, the pore size distributions shifted to lower values with the decrease of the IS of the solution (Fig. 8). Consequently, the mean pore size decreased from 25.9 ± 8.4 and 66 ± 17 μm at IS = 10^{-7} mol/L to 6.6 ± 2.1 and 29 ± 11 μm at IS = 10^{-1} mol/L for $SMA_{0.25}$ to $SMA_{0.5}$, respectively (Figs. 8).

DISCUSSION

Hydrogels are hydrophilic materials that are able to change their volume when they are in contact with specific solvents. Because of this peculiarity, these materials have been proposed for a large number of applications, including functional membranes and biochemical devices.[2,4] Furthermore, when prepared starting from biocompatible materials, hydrogels may be successfully used as tissue engineering scaffolds and controlled drug-delivery platforms.[5,6,8,9]

TABLE II
Results of the TGA and DSC Characterizations Performed on the Swollen Hydrogels

Sample	30–150°C weight loss (%)	T_f (°C)	ΔH_m (J/g)	$W_{H2O}{}^f/W_G$		$W_{H2O}{}^b/W_G$	
				S_w	TGA	S_w	TGA
SM	98.1	2.36	307.4	61.2	48.5	4.2	3.1
$SMA_{0.25}$	98.9	1.60	320.2	99.4	157.7	3.8	2.4
$SMA_{0.5}$	99.6	0.28	330.3	264.1	247.6	1.6	1.4

S_w, swollen weight.

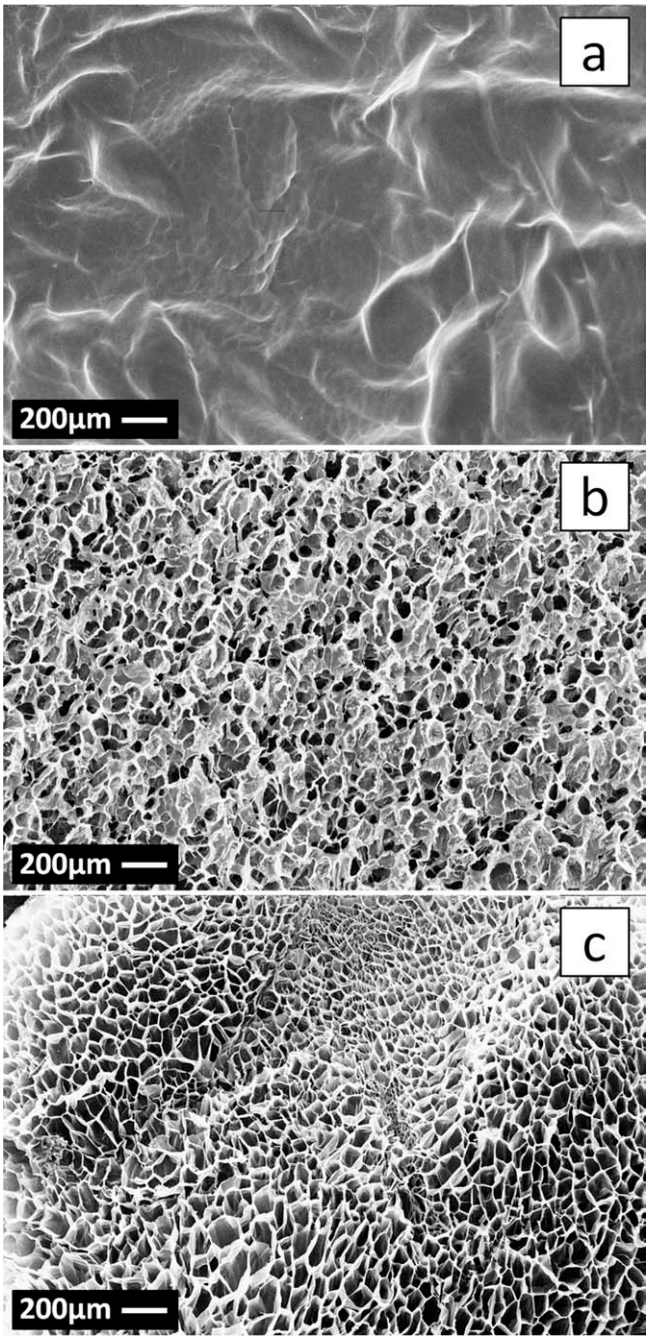

Figure 6 (a) SM, (b) $SMA_{0.25}$, and (c) $SMA_{0.5}$ morphologies at the equilibrium in 10^{-7} IS solution.

Hydrogel performances are strongly dependent on their physical and chemical properties, which therefore, need to be finely controlled for practical use.

The preparation of porous hydrogels with different pore structure features, at both micrometric and nanometric pore size scales, have been investigated with several approaches, such as gas foaming, phase separation, freeze-drying, and reverse-casting techniques.[4,10,12–15] These studies showed that the porosity within the hydrogels allowed for a faster and more controlled volume change in response to specific external milieus. Indeed, the porous network may allow for the solvent to flow simultaneously by convection and diffusion, finally reducing the swelling time and enhancing solvent uptake.[4,10,12–15] Furthermore, the presence of an interconnected porosity is also strongly required for biomedical purposes because of the need to promote and guide cell infiltration in three dimensions and because of the improvement of the sequestration and release of bioactive moieties.[5,12]

In this work, we report the fabrication of porous polyacrylamide hydrogels via reverse casting, and we critically investigated the correlation between the morphology, thermal properties, and swelling behavior of the hydrogels.

As reported in the scheme of Figure 1, the porous hydrogels were prepared with an agarose gel as a templating agent, and two different templating solution concentrations were selected to control the pore structure features. The selection of the agarose as a templating agent mainly relied on the inherent properties of the agarose/water solutions and gels. Indeed, depending on the concentration of the polymer, the agarose may have been able to undergo a reversible sol–gel transition by a simple change in the temperature of the system. Furthermore, as qualitatively shown in the SEM micrograph of Figure 2, in the gel state, the agarose evidenced a morphology characterized by a highly interconnected fibrillar network and, therefore, may have been able to accommodate the monomer solution well during gelification. After the setting of the chemical gel (Fig. 1), we obtained an interpenetrated system consisting of a chemical gel and a thermoreversible gel, from which it was further possible to selectively extract the agarose by simply increasing the temperature. A similar system was very recently reported by Fernández et al., who investigated the effect of the composition of the agarose gel on the morphology and viscoelastic properties of interpenetrated hydrogels of agarose and polyacrylamide. According to our results (Fig. 2), in their study, the authors observed a morphology that corresponded to a network of intertwined fibrils of agarose, and the extent of the fibril network increased with the increase of the agarose concentration. Nevertheless, in contrast to their study, in this work, we mainly focused on the possibility of selectively extracting the agarose fibrils from the interpenetrated network to create porous polyacrylamide hydrogels with well-controlled porosity patterns and, therefore, improved swelling capabilities.

The results of the morphological characterization performed on the hydrogels in the dry conditions (Fig. 4) and wet conditions (Figs. 6 and 7) confirmed the efficacy of the developed approach for the creation of porous polyacrylamide hydrogels, whereas the swelling results (Fig. 5) indicate a direct

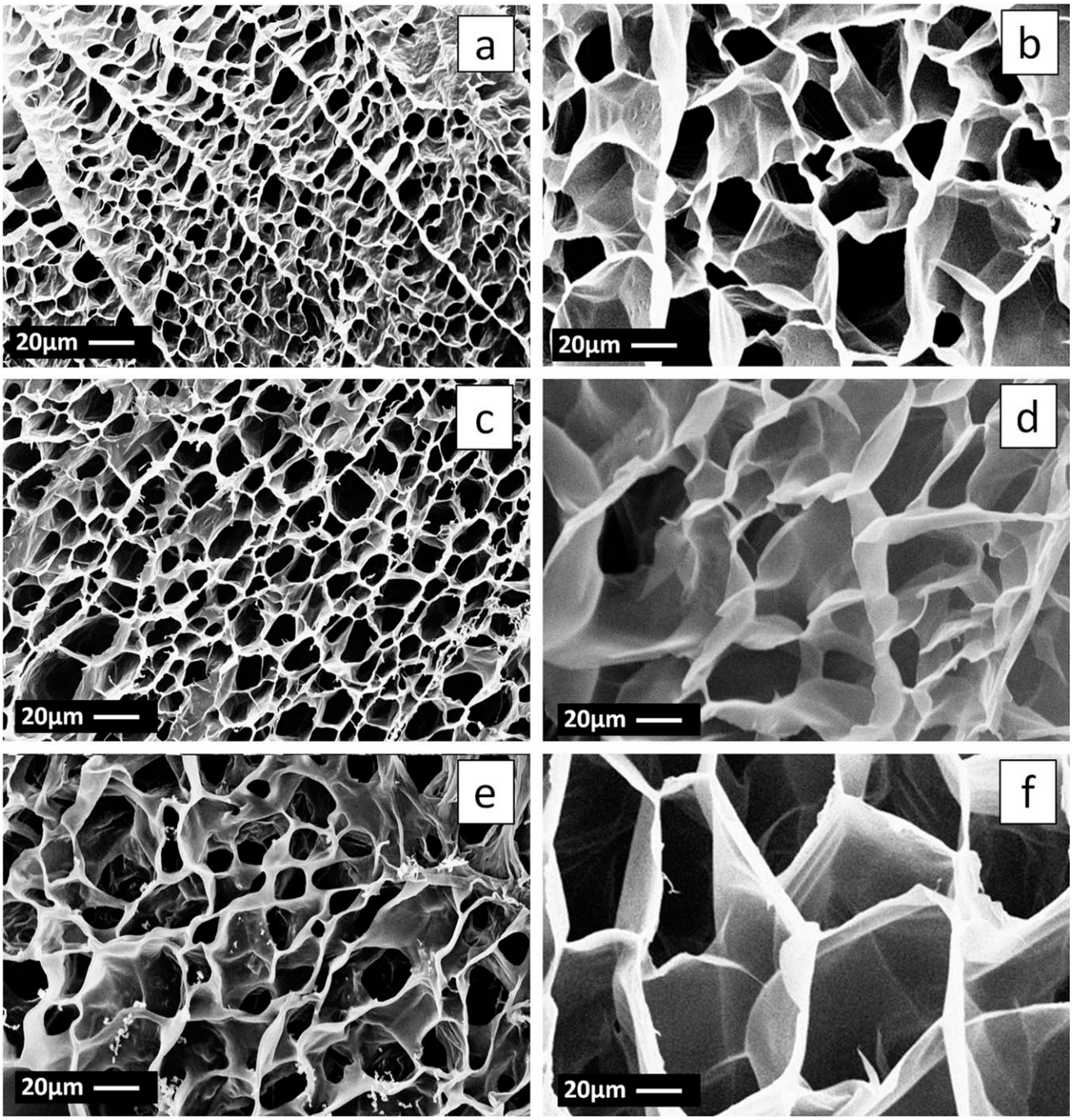

Figure 7 Effect of the IS of the solution on the morphology of $SMA_{0.25}$ (left column) and $SMA_{0.5}$ (right column) at the equilibrium: (a,b) 10^{-1}, (c,d) 10^{-4}, and (e,f) 10^{-7}.

correlation between the sample's microstructure and swelling. In particular, in contrast to the untreated SM hydrogel, which showed a nonporous surface in both the dry state [Fig. 4(a)] and swollen state [Fig. 6(a)], the hydrogels synthesized by the reverse-casting approach were characterized by highly ordered pore structures [Fig. 6(b,c)] and improved swelling behavior (Fig. 5). Although several approaches have been reported for the creation of porous hydrogels,[6,12–15] the use of agarose as a templating agent may provide several advantages. First, the agarose was able to create an interpenetrated network in water solutions at very low polymer concentrations (as low as 5×10^{-3} w/v, as in the case of $SMA_{0.25}$). This property allows for the achievement of the percolation of the porogen without the use of a high amount of templating agent, as otherwise necessary in the case of microparticulate templating agents. Furthermore, the biocompatibility of the agarose ensured that the presence of polymeric residues

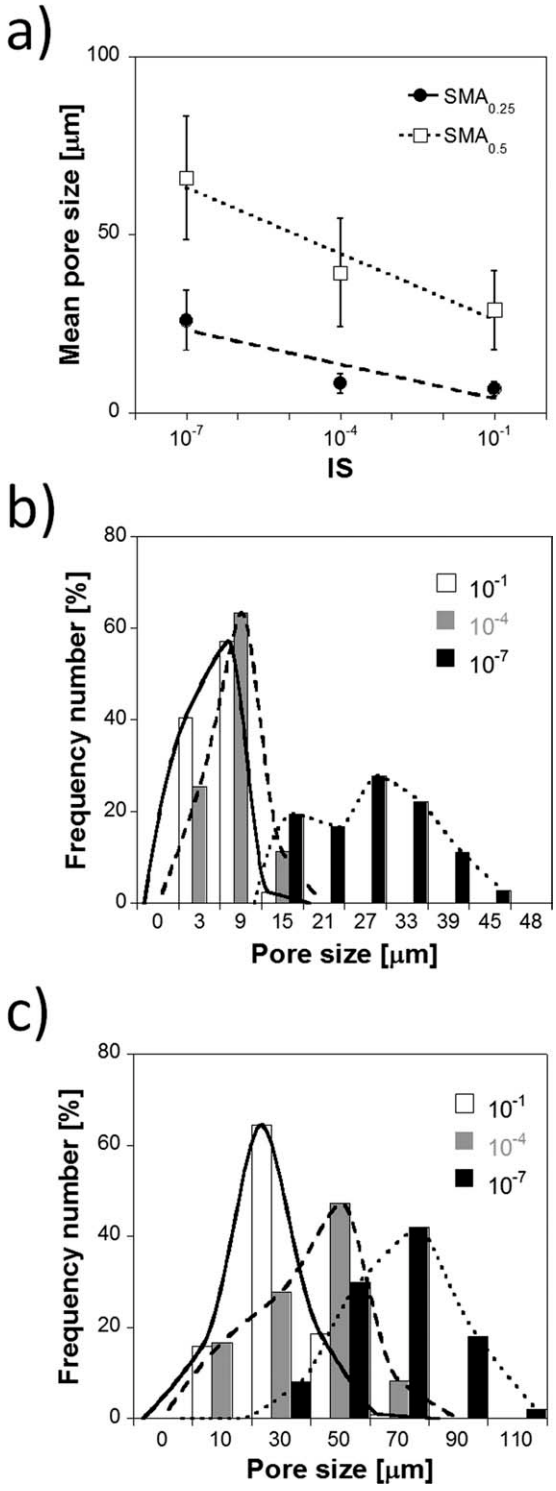

Figure 8 (a) Effect of the IS of the solution on the mean pore size of the $SMA_{0.25}$ and $SMA_{0.5}$ hydrogels at equilibrium. The effect of IS of the solution on the pore-size distribution of (b) $SMA_{0.25}$ and (c) $SMA_{0.5}$ at equilibrium.

within the hydrogel after the reverse-casting process would not produce a cytotoxic effect in the case of tissue engineering applications.

As expected, the swelling ratio of all of the hydrogels progressively decreased with the increase of the IS of the solution because of the reduced water activity of the salt solutions and because of the shielding effect exerted by Na^+ and Cl^- ions on the polymeric bulk charges. Similar results were reported by Baker et al.[18] for acrylamide-based polyampholyte hydrogels and Zhang and Peppas[19] for poly(methacrylic acid)/poly(*N*-isopropylacrylamide) interpenetrating systems.

These results were also confirmed by the observed increase of the mean pore size with the increase of the agarose concentration and the decrease of IS as a consequence of the reduced capability of the porous network to allow for solvent diffusion, as previously discussed.

The morphological characterization of the dry hydrogels suggested that the pore structure features of the $SMA_{0.25}$ and $SMA_{0.5}$ samples did not completely resemble the fibrillar structure of the agarose (cf. the SEM micrograph of Figs. 4 and 6 with the SEM micrograph of Fig. 2). It is important to point out that the gelification process of the agarose solution in the presence of the monomer solution did not induce changes in the fibrillar morphology of the agarose gel (data not shown). Therefore, this difference was probably ascribable to the fact that the agarose gelification occurred when the chemically synthesized gel was in a partially swollen state and was, therefore, different from the dry and swollen conditions of the morphological analysis.

The enhancement of the swelling ratio observed after the reverse-casting process may have not only been related to the observed differences in the microstructural properties of the hydrogels but should have also been ascribable to the effect of the reverse-casting process on their thermal properties. Indeed, the ability of a hydrogel material to swell is not only related to its morphological features[10,11] but is also strongly dependent on the elastic properties of the polymeric network.[20–23] By considering that the chemical structure of the hydrogels was not significantly affected by the reverse-casting process (Fig. 3), we believe that the enhanced swelling capability of $SMA_{0.25}$ and $SMA_{0.5}$, when compared to neat SM, was also related to the higher chain mobility of the polymer network, as indicated by the decrease of the values of T_g in the case of porous hydrogels (Table I). The decrease of T_g of the hydrogels may be explained by the fact that during mixing, the agarose solution led to a partial dilution of the monomer solution. This effect may have also been responsible for the observed decrease of the degradation temperatures of both the $SMA_{0.5}$ and $SMA_{0.25}$ samples when compared to neat SM (Table I). Similar results were reported by Wieczorek et al.[21] for hydrogels prepared by the mixture of acrylamide with agar; this, finally, suggests the key role of the agarose solution on the plasticization of the polymer network.[21]

The thermal characterization results of the swollen hydrogels, reported in Table II, supported the swelling results of Figure 5 (cf. the weight losses of the

hydrogels in the 30–150°C temperature range) and allowed the assessment of the amount of freezable and nonfreezable water within the different samples. In particular, the DSC ice-melting results showed the increase of the melting point from 2.36°C for neat SM to 0.28°C for $SMA_{0.5}$ as a consequence of the increase of W^f_{H2O}/W_G and the concomitant decrease of W^b_{H2O}/W_G (Table II). Similar results were reported by Li et al.[16] for poly(vinyl alcohol) hydrogels; this confirmed that the capillary diffusion of the solution within the hydrogels played a key role in their swelling properties.

CONCLUSIONS

In this work, we report the design and fabrication of porous polyacrylamide hydrogels via a thermal reverse-casting technique. This technique involved the polymerization of a monomer solution within the space of a thermoreversible gel of agarose, which after the setting of the chemical gel, was removed to allow for the creation of an interconnected porosity pathway. Two different templating solution concentrations were selected to control the pore structure features and the swelling behavior of the hydrogels.

The results of this study demonstrate that the proposed technique allowed the fabrication of porous polyacrylamide hydrogels with well-controlled morphologies and pore structures and, therefore, improved the solvent-retaining capability compared to a nonporous structure.

The authors gratefully acknowledge Luciano Rosato for his support in the hydrogel preparation and Letizia Verdolotti for helping out with Fourier transform infrared analysis.

References

1. Almdal, K.; Djre, J.; Hvidt, S.; Kramer, O. Polym Gels Net 1993, 1, 5.
2. Miyata, T.; Asami, N.; Okawa, K.; Uragami, T. Polym Adv Technol 2006, 17, 794.
3. Kim, S. J.; Park, S. J.; Kim, S. I. React Funct Polym 2003, 55, 61.
4. Ulbricht, M. Polymer 2006, 47, 2217.
5. Drury, J. L.; Mooney, D. J. Biomaterials 2003, 24, 4337.
6. Bajpai, A. K.; Shukla, S. K.; Bhanu, S.; Kankane, S. Prog Polym Sci 2008, 33, 1088.
7. English, A. E.; Mafé, S.; Manzanares, J. A.; Yu, X.; Grosberg, A. Y.; Tanaka, T. J Chem Phys 1996, 104, 8716.
8. Rosso, F.; Barbarisi, A.; Barbarisi, M.; Petillo, O.; Margarucci, S.; Calarco, A.; Peluso, G. Mater Sci Eng C 2003, 23, 371.
9. Burnham, M. R.; Turner, J. N.; Szarowski, D.; Martin, D. L. Biomaterials 2006, 27, 5883.
10. Ceylan, D.; Ozmen, M. M.; Okay, O. J Appl Polym Sci 2006, 99, 319.
11. Lu, G. D.; Yan, Q. Z.; Ge, C. C. Polym Int 2007, 56, 1016.
12. Sannino, A.; Netti, P. A.; Madaghiele, M.; Coccoli, V.; Luciani, A.; Maffezzoli, A.; Nicolais, L. J Biomed Mater Res A 2006, 79, 229.
13. Přádný, M.; Lesný, P.; Smetana, K., Jr.; Vacík, J.; Šlouf, M.; Michálek, J.; Syková, E. J Mater Sci Mater Med 2005, 16, 767.
14. Kato, N.; Gehrke, S. H. Colloids Surf B 2004, 38, 191.
15. Sannino, A.; Netti, P. A.; Mensitieri, G.; Nicolais, L. Compos Sci Tech 2003, 63, 2411.
16. Li, W.; Xue, F.; Cheng, R. Polymer 2005, 46, 12026.
17. Fernández, E.; Mijangos, C.; Guenet, J.; Cuberes, M. T.; López, D. Eur Polym J 2009, 45, 932.
18. Baker, J. P.; Stephens, D. R.; Blanch, H. W.; Prausnitz, J. M. Macromolecules 1992, 25, 1955.
19. Zhang, J.; Peppas, N. A. Macromolecules 2000, 33, 102.
20. Pooley, S. A.; Rivas, B. L.; Cárcamo, A. L.; Pizarro, G. Polym Bull 2009, 62, 469.
21. Wieczorek, W.; Florjanczyk, Z.; Stevens, J. R. Electr Acta 1995, 40, 2327.
22. Gundogan, N.; Okay, O.; Oppermann, W. Macromol Chem Phys 2004, 205, 814.
23. Aroca, A. S.; Fernández, A. J. C.; Ribelles, J. L. G.; Pradas, M. M.; Ferre, G. G.; Pissis, P. Polymer 2004, 45, 8949.